Hindawi Publishing Corporation
ISRN Nanomaterials
Volume 2013, Article ID 208614, 7 pages
http://dx.doi.org/10.1155/2013/208614

Research Article

Temperature Effects on the Crystallization and Coarsening of Nano-CeO_2 Powders

H. F. Lopez and H. Mendoza

Department of Materials Science and Engineering, CEAS, University of Wisconsin-Milwaukee, 3200 N. Cramer Street, Milwaukee, WI 53211, USA

Correspondence should be addressed to H. Mendoza; humberto@uwm.edu

Received 22 July 2013; Accepted 18 August 2013

Academic Editors: R. Hong, Z. Jiang, and A. V. Raghu

The effect of temperature on nano-CeO_2 particle coarsening is investigated. The nanoceria powders were synthesized using the microemulsion method and then exposed to temperatures in the range of 373–1273 K. It was found that the nanoparticles exhibited a strong tendency to form agglomerates and through the application of ultrasound these agglomerates could be broken into smaller sizes. In addition average nanoparticle sizes were determined by powder X-ray diffraction (XRD). The outcome of this work indicates that the initial nano-CeO_2 powders are amorphous in nature. Annealing promotes CeO_2 crystallization and a slight shift in the (111) XRD intensity peaks corresponding to CeO_2. Moreover, at temperatures below 773 K, grain growth in nano-CeO_2 particles is rather slow. Apparently, mass transport through diffusional processes is not likely to occur as indicated by an estimated activation energy of 20 kJ/mol. At temperatures above 873 K, the measured activation energy shifted to 105 kJ/mol suggesting a possible transition to Ostwald-Ripening type mass transport mechanisms.

1. Introduction

Nanocrystalline ceria possesses unique properties which enable it to be widely used in various industrial applications. Among the different uses of nanoceria are acting as coatings for high temperature oxidation protection in alloys [1–4], acting as catalysts and gas sensors [5, 6], being used for absorption and redistribution of UV radiation, [7]. Typical applications involve high temperature exposure above 873 K. Under these conditions mass transport mechanisms become active, particularly oxygen anions due to their inherently high mobility in the nanoceria crystal lattice [8]. In contrast, the diffusivity of cerium ions does not seem to be significant at these temperatures, but there is no data available on actual diffusivity values. Despite the lack of diffusivity data, it is expected that the nanosized CeO_2 particles will exhibit appreciable coarsening upon exposure to elevated temperatures.

Coarsening in nanoparticle dispersions at high temperatures is typically driven by chemical potential differences associated with curvature effects on the particle interfacial energies. This phenomenon, known as Ostwald-Ripening (O-R), has been widely investigated in conventional materials exposed to high temperatures [9, 10]. From the published literature [11], it is apparent that O-R also occurs in nanometallic and nanoceramic compounds. Eastman [12] reported grain growth exponents, n of approximately 3 in nano-TiO_2 or in yttria-stabilized nano-ZrO_2 systems indicating that O-R might be the dominant coarsening mechanism.

Although there are very limited published works on the coarsening of CeO_2 nanopowders, direct experimental evidence has been reported by Ivanov et al. [13]. In their work, they investigated nanoceria particle coarsening at temperatures as high as 973 K. From their experimental outcome, they found that coarsening in this temperature regime occurs as a result of cooperative mass transfer processes involving mutual movement and rotation of CeO_2 crystallites.

Apparently, mass transfer through thermally activated diffusion processes does not play an important role in the coarsening of the CeO_2 particle agglomerates at temperatures below 973 K. Nevertheless, from their work, it is not clear whether the same mechanism will be prevalent above 973 K. Among the applications of nano-CeO_2 particles are their potential use as coatings for oxidation protection in stainless steels at temperatures up to 1273 K [3, 4]. Thus, it is plausible

that at elevated temperatures diffusional processes might become dominant in the coarsening of CeO_2 particle agglomerates. Accordingly, the present work further investigates coarsening in nanoceria powders when they are exposed to temperatures in the 473–1273 K range.

2. Experimental

Preparation of a size dispersion of nanoceria particles was achieved by using the microemulsion method [14, 15]. The starting materials employed consisted of (a) cerium nitrate hexahydrate ($Ce(NO_3)\cdot 6H_2O$), (b) water and (c) hydrogen peroxide (H_2O_2). All the chemicals and reagents were purchased from Aldrich Chemicals Company, Inc. The nanoceria powders were produced by dissolution of cerium nitrate (0.1085 g) in 25 mL of distilled deionized water and then stirring for 1 hour. This was followed by adding hydrogen peroxide in a dropwise mode (10 mL). The reaction was allowed to take place for 2 hours. Afterwards, the precipitate was collected, washed with water, and calcinated at 573 K for 60 minutes. In this process the synthesis mechanism can be described by the following reactions [15].

Cerium nitrate dissociation in water:

$$Ce(NO_3)_3 \xleftrightarrow{H_2O} Ce^{3+} + 3(NO_3)^-. \quad (1)$$

Reduction of dissolved oxygen

$$O_2\,(aq) + 2H_2O + 4e^- \longrightarrow 4OH^-\,(aq), \quad (2)$$

$$O_2\,(aq) + 2H_2O + 2e^- \longrightarrow H_2O_2\,(aq) + 2OH^-\,(aq), \quad (3)$$

$$4Ce^{3+}\,(aq) + O_2\,(aq) + 4OH^-\,(aq) + 2H_2O \longrightarrow 4Ce(HO)_2^{2+}\,(aq), \quad (4)$$

$$2Ce^{3+}\,(aq) + H_2O_2\,(aq) + 2OH^-\,(aq) \longrightarrow 2Ce(OH)_2^{2+}\,(aq). \quad (5)$$

Precipitation of $Ce(OH)_2^{2+}$ from reactions (4) or (5) as insoluble CeO_2 occurs as

$$Ce(OH)_2^{2+}\,(aq) + 2OH^-\,(aq) \longrightarrow Ce(OH)_4\,(s) \longrightarrow CeO_2\,(s) + H_2O. \quad (6)$$

The transformation of $Ce(OH)_4(s)$ into $CeO_2(s)$ after heating at 573 K for 60 minutes (see (6)) is illustrated in Figure 1. This reaction was confirmed by XRD determinations of the $CeO_2(s)$ compound and by the typical "pale yellow" coloration reported for this compound [14, 15]. The synthesized cerium oxide nanoparticles were then collected and suspended in distilled water to have a 10 wt% $CeO_2(s)$ concentration solution.

X-ray diffraction was used for phase identification and also for identification of the level of crystallinity in the nanoceria particles. Accordingly, double angle XRD with unresolved Cu Kα radiation in the 2θ range of 5° to 75° was used here. High resolution scans were implemented for accurate determinations of the relative positions of the principal intensity peaks corresponding to the ceria nanoparticle films.

The effective sizes of the cerium oxide were determined using the light scattering technique in a Malvern instrument, Zetasizer Nano ZS. In this work, "effective sizes" referred to the size of the nanoceria particle clusters as they were influenced by temperature, without considering individual nanoparticle sizes. Moreover, the effect of ultrasound on the resultant cluster sizes was considered. Nanoceria particle crystallization and coarsening were investigated by annealing the synthesized ceria at 373 to 1073 K for 1 hour. This was followed by measuring particle sizes by X-ray diffraction after high temperature exposure using coherent scattering lengths according to the Selyakov-Scherrer relationship:

$$d = \frac{K\lambda}{\beta \cos\theta}, \quad (7)$$

where K is the shape factor, λ is the X-ray wavelength, β is the full width for the half maximum intensity for the intensity peak, and θ is the Bragg angle. Corrections due to instrumental broadening effects, β_{inst} were made by employing a Gaussian-Gaussian relationship:

$$\beta^2 = \beta_{total}^2 - \beta_{inst}^2, \quad (8)$$

where β_{total} is the total full width for the half maximum intensity of the (111) peak for ceria. In addition, atomic force microscopy (AFM) and scanning electron microscopy (SEM) were used for the characterization of the cerium oxide cluster dispersions and morphology.

3. Results and Discussion

The resultant cerium oxide nanoparticles produced by the microemulsion method were found to be amorphous in nature. Figure 2 shows broad, low resolution XRD peak scans from the collected powders, including the quartz substrate. In this figure, the vertical dotted line indicates 2θ positions corresponding to the (111) plane for crystalline CeO_2. In particular, notice that the shape of the XRD intensity curve indicates that the initially collected powders are amorphous in nature. From this figure it is evident after annealing at the various temperatures (373–773 K) for 60 minutes that powders become increasingly crystalline. At 473 K the XRD intensity peak (111) corresponding to Ce_2O ($2\theta = 28.6°$) starts to develop indicating crystallization of the nanoceria particles. Annealing at temperatures above 473 K gives rise to the development of XRD intensity peaks corresponding to the (200) and (220) Ce_2O planes at $2\theta = 33.1°$ and $2\theta = 47.4°$, respectively.

In addition, the peak amplitude consistently increases while peak broadening is sharply reduced at increasing temperatures and at 773 K most of the nanoceria powders are fully recrystallized. Recrystallization of nano-CeO_2 at 573 K has also been reported by Ivanov et al. [13]. In their work, a well-defined exothermal was found in the experimental DTA curves that can be attributed to CeO_2 recrystallization and to the decomposition of any residual cerium compounds. A close examination of the XRD intensity peaks (111) and (200) developed (2θ from 25° to 35°) in the powders annealed at 373–1073 K is shown in Figure 3. From this figure it is

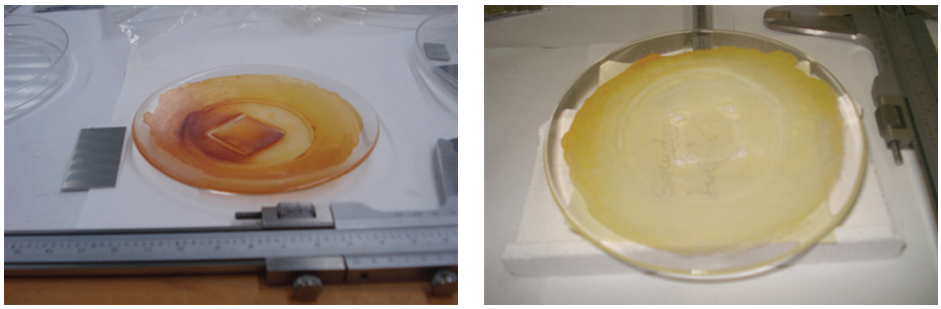

(a) (b)

FIGURE 1: (a) $Ce(OH)_4$(s) precipitated just after the drying stage and (b) nanocrystalline CeO_2 after annealing at 573 K for 60 minutes.

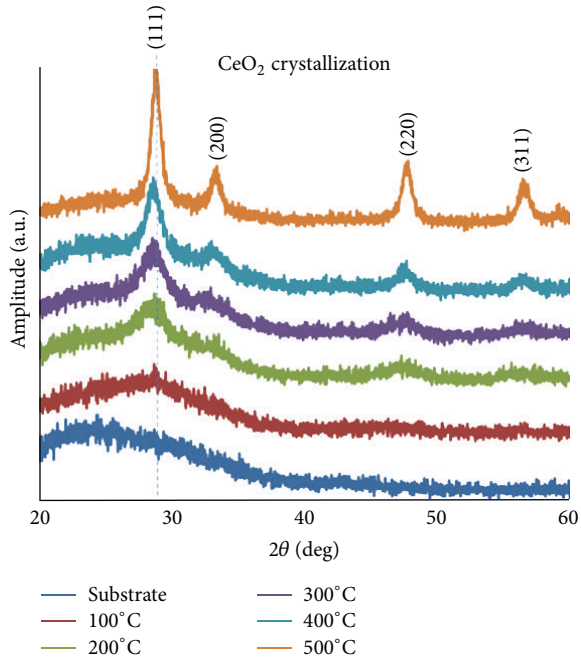

FIGURE 2: XRD intensity peaks from precipitated powders showing the effect of temperature on the transition from amorphous to crystalline nano-CeO_2.

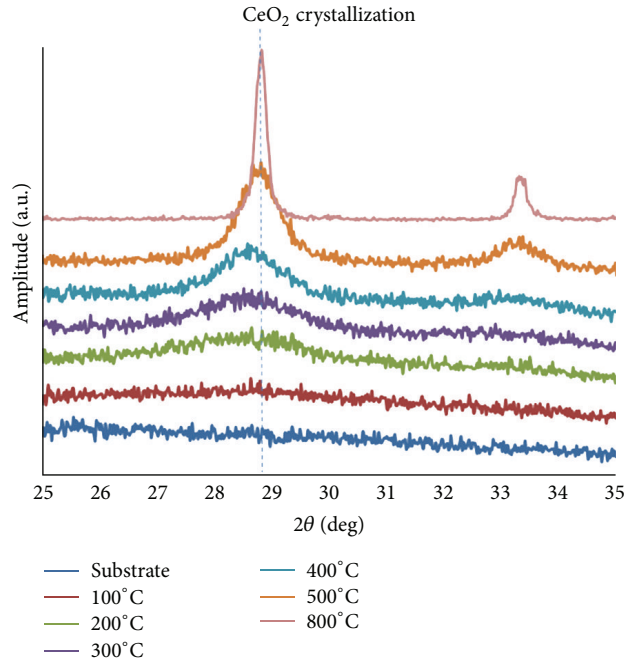

FIGURE 3: XRD intensity peaks associated with the recrystallization of CeO_2 powders and the effect of temperature on peak shifting and broadening.

evident that peak broadening continues to decrease and that maximum peak intensity occurs at 1073 K.

In addition, notice that there is a slight shift of the (111) intensity peaks towards the right (diffraction angle, $2\theta = 28.6$) after exposure to increasing temperatures. This effect can be related to a reduction in the actual interplanar (111) spacings as the effective particle size increases with the annealing temperatures. It is well known that, when CeO_2 crystallites reach sizes of less than 5 nm, Ce^{+3} ions and oxygen vacancies are induced in the CeO_2 particles giving rise to crystal lattice expansions [16, 17]. Thus, the shifting in diffraction peak positions can be attributed to the removal of any crystal lattice expansions as a result of nanoceria coarsening. Alternatively, rearrangement of the atom periodicity during the transformation from amorphous to crystalline CeO_2 might also contribute to this shifting effect.

3.1. Nanoceria Cluster Sizes. The effective size of cerium oxide nanoparticle clusters was measured using a light scattering technique. By "effective size," we mean that only the size of the agglomerates was measured without detecting single nanoparticle sizes. The nanoceria cluster sizes were measured after calcination of the synthesized nanoceria at 573 K for 3 hours. Figure 4(a) gives a statistical distribution of the effective sizes of agglomerated nanocrystalline cerium oxide particles. Also, Figure 4(b) shows the statistical distribution of the same particles after exposure to ultrasound vibration for 10 minutes. Notice that the ultrasonic dispersion reduces the effective size of the agglomerates from 390 nm to 170 nm.

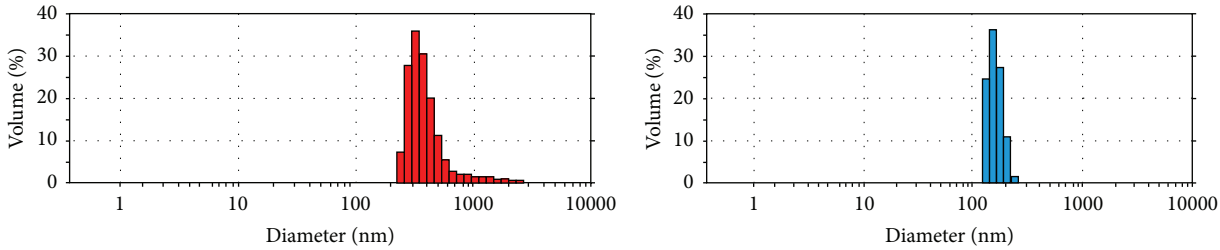

Figure 4: (a) Size distribution of nano-CeO_2 agglomerates after precipitation synthesis and (b) after 10 minutes of ultrasonic dispersion.

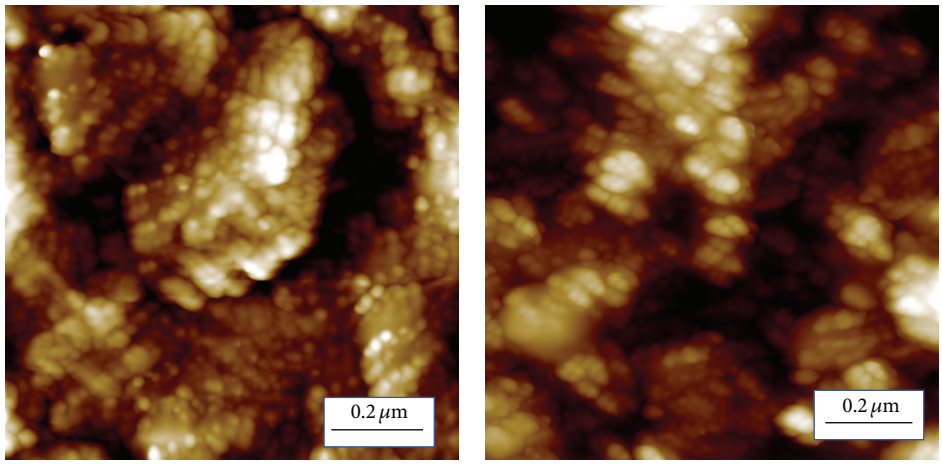

Figure 5: AFM micrographs showing (a) morphology of the as-synthesized nano-CeO_2 particle agglomerates and (b) effect of the ultrasonic dispersion on breaking the particle clusters.

Nevertheless, it was found that after 10 minutes of ultrasonic treatment the effect is reversed and the effective size of particle agglomerates tends to increase.

Atomic force microscopy (AFM) was used for further confirmation of the morphology and distribution of the nanoceria agglomerates. Figures 5(a) and 5(b) are AFM micrographs on a 1 micron square area containing nanoceria clusters indicating the morphology and size of the synthesized cerium oxide clusters. In turn, this agrees with the determinations of effective nanoparticle sizes for the agglomerated particles found using the light scattering method (390 nm). It also agrees with the effect of ultrasonic treatment on breaking down cluster sizes (down to 170 nm).

3.2. CeO_2 Particle Coarsening. Particle coarsening can be inferred from the experimental determinations of particle size using Scherrer equation (7) at the various annealing temperatures. Figure 6 shows particle coarsening as a function of temperature and for comparison purposes it includes data from Ivanov et al. work [13]. From this figure, it is evident that coarsening at temperatures below 773 K is rather sluggish, (i.e., average particle size only increases from 3.5 nm to 9.7 nm). At temperatures between 773 and 1073 K growth is accelerated as particle sizes increase from 9.7 nm to 48 nm,

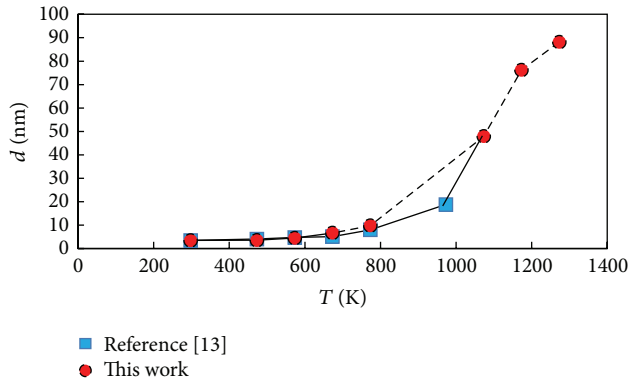

Figure 6: Average sizes of nano-CeO_2 particles after annealing at 373 K–1273 K for 1 hour. The graph includes data from the work of Ivanov et al. [13].

while at 1173 K growth is greatly enhanced as particle sizes increase from 48 nm to 76.2 nm in a 100 K interval. At 1273 K, particle coarsening exhibits significant attenuation as the incremental particle size is only 12 nm.

From the experimental outcome, it is apparent that there are three plausible coarsening regimes. At low temperatures,

coarsening is severely limited by thermally activated mechanisms such as a threshold for crystallite intergrowth or by limited diffusional mass transport at temperatures below 573 K. In the work of Ivanov et al. [13], the barrier for particle coarsening in CeO_2 crystallites was attributed to various surface defects present in the agglomerates. The dominant defects that act as coarsening barriers include porosity [18] and contacts with other particles, as well as the substrate, all of which inhibit the free movement/rotation of the crystallites relative to one another. This is supported by the development of a bimodal distribution of pores in the agglomerates and a low densification in the powder structure [19].

From the work of Ivanov et al. [13], it is evident that at temperatures in the range of 773–1073 K, thermally activated processes such as crystallite rotation and alignment become dominant. In addition, the developed bimodal pore distribution tends to disappear. As pore closure occurs, with only isolated pores, grain growth through mass transport becomes unrestricted [20]. In turn, this suggests that the pinning effect of open porosity barriers that hinder grain coarsening tends to be eliminated at increasing temperatures. Further confirmation is found by the development of a bimodal distribution of nanoceria crystallites which also tends to fade away at increasing temperatures.

The development of bimodal particle distributions can also be explained by limiting cases of the classic Ostwald-Ripening theory [9, 10]. Apparently, at low coarsening temperatures, nucleation of new rows of atoms in growing nanoparticles at faceted interfaces might be rate limiting. Incubation times for nucleation can be relatively long and it is plausible that other mechanisms such as particle rotation and particle alignment become dominant resulting in particle intergrowth. Nevertheless, from the work of Wynblatt and Gjostein [9], it is clearly predicted that at increasing temperatures the bimodal particle distribution disappears as the incubation times for nucleation of rows of atoms on faceted interfaces are greatly reduced.

From the outcome of this work, it is evident that similar particle coarsening mechanisms to the ones observed by Ivanov et al. [13] are active all the way to 973 K (see Figure 6). Nevertheless, above 973 K, grain coarsening is significantly enhanced suggesting a shift in grain coarsening to classic O-R mass transport as reported for other systems [9, 10]. In general, grain coarsening can be described by the equation

$$d^n - d_o^n = Kt, \tag{9}$$

where d is the average particle size, d_o is the initial particle size, n is the particle growth exponent, K is a constant which depends on temperature ($K = K_o \exp(-Q/RT)$) and t is time. From this expression, high values of n indicate a rather sluggish crystallite growth due to restricted boundary mobility and they are consistent with the experimental outcome for low temperature particle coarsening [11, 21]. Equation (9) can be simplified to the form $d = K't^m$ where $m = 1/n$ and the m exponent can be graphically found from a logarithmic plot of d versus t as shown in Figure 7. Notice from this figure that the m exponent is relatively low ($m = 0.0397$ at 673 K) but it tends to increase as temperature increases.

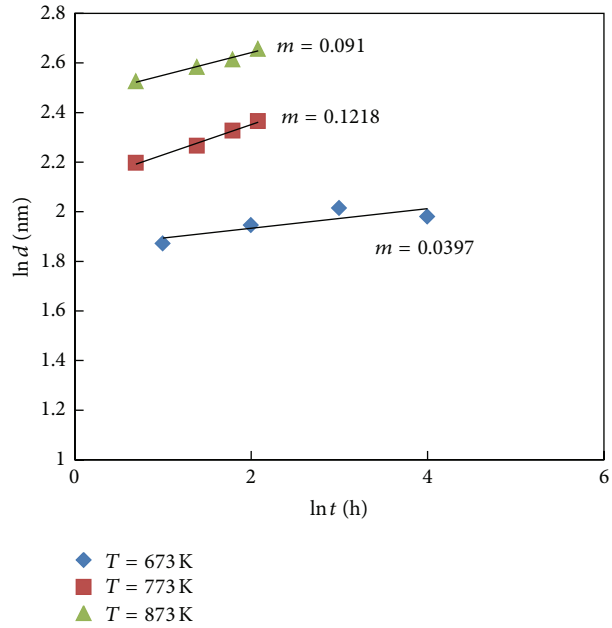

Figure 7: Power exponents; n found from the work of Ivanov et al. [13] for nano-CeO_2 grain growth in the temperature range of 673–873 K and for times up to 8 hours.

In addition, activation energies can be estimated from the K values found at the line intercepts in Figure 7. In turn, the activation energy in this temperature range yielded values of only 20 kJ/mol as shown in Figure 8. The relatively low magnitudes of the exhibited activation energies strongly support the observations of crystallite maneuvers such as rotation and alignment, rather than diffusion controlled mass transport mechanisms.

Since there is no available experimental information that can be used to estimate n values at temperatures above 973 K, a value of $n = 3$ typical of O-R mechanisms was assumed for high temperature particle coarsening. This can be justified by the clear tendency for n values to drop at increasing temperatures (Figure 8). Moreover, it is expected that at temperatures above 1/3 of the melting temperature, mass transport by diffusional mechanisms becomes important in solids at the grain boundary interfaces [22]. Figure 9 is an Arrhenius plot of $\ln(d^3 - d_o^3/t)$ versus $1/T$ in the temperature range of 1073–1273 K. From this plot, activation energies of 105 kJ/mol are found which might be related to grain boundary Ce^{+4} ion transport.

Nevertheless, an actual grain coarsening mechanism cannot be established as the actual n values are not known and they can be strongly influenced by impurity and porosity levels in the nanoceria agglomerates. From the work of Thuenissen et al. [23], solute drag effects through the action of dopants such as Ca in CeO_2 nanoparticles severely hinder coarsening. In this work the addition of 6% Ca was sufficient to retain a 30 nm CeO_2 particle size all the way to 1625 K after full sintering. The experimental activation energies obtained in this work are of the order of 105.2 kJ/mol but they cannot be attributed to a particular mechanism as there are no

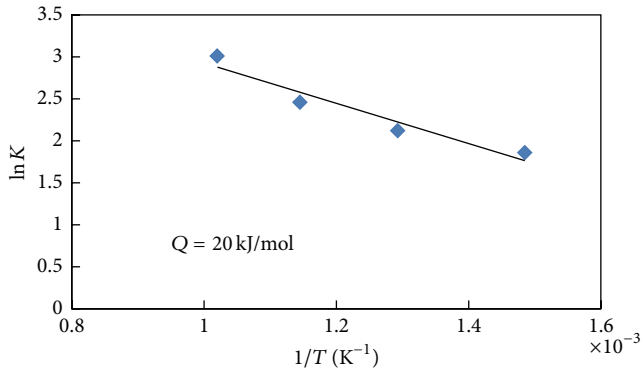

FIGURE 8: Arrhenius plot of CeO_2 nanograin size versus $1/T$ showing the exhibited activation energy at low temperatures (673 K to 973 K) using data from Ivanov et al. [13].

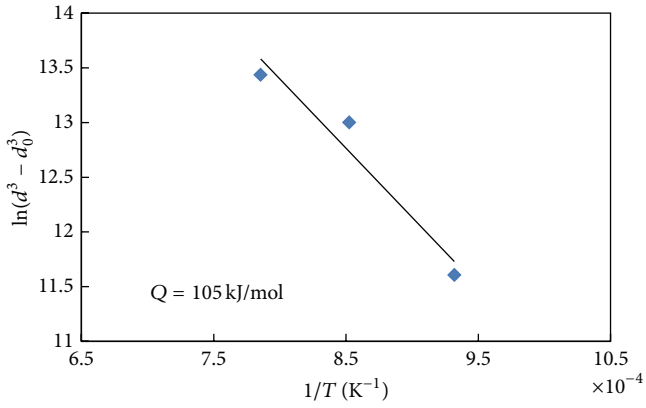

FIGURE 9: Arrhenius plot of CeO_2 nano-grain size versus $1/T$ showing the exhibited activation energy in the temperature range of 1073 K to 1273.

diffusional data reported for either gb or bulk diffusion in CeO_2. In nanoparticle coarsening relatively low activation energies have been reported in the literature [11, 24]. Also, in the work of Eastman [12], activation energies of 83 kJ/mol are reported for grain growth in nano-TiO_2, but no mechanisms have been proposed based on these results.

Finally, the experimental outcome indicates that at 1273 K crystallite coarsening seems to be severely attenuated. Apparently, net crystallite coarsening is influenced by possible mass losses through ceria evaporation processes just as the ones reported for chromia scales [24]. In turn, the volume fraction of crystallite CeO_2 can be significantly reduced, thus influencing net coarsening. However, there are no published reports on possible CeO_2 evaporation reactions that will allow to establish whether these mechanisms play a role during high temperature sintering.

4. Conclusions

Nanoceria powders were synthesized using the microemulsion method. The initially synthesized nanoceria particles were prone to form agglomerates and ultrasound was found to be somewhat effective in reducing the agglomerate sizes. The average nanoceria particle sizes were determined using powder X-ray diffraction (XRD). The grain coarsening kinetics was investigated by exposing the nano-CeO_2 powders to 373–1273 K for up to one hour. The outcome of this work can be summarized as follows.

(1) The initial nano-CeO_2 powders are amorphous in nature, but heating at temperatures of up 773 K promotes CeO_2 crystallization. This is concomitant with a slight shift in the CeO_2 (111) XRD intensity peaks.

(2) Below 773 K, grain growth in nano-CeO_2 particles is rather sluggish. This is attributed to the presence of porosity and other defects which effectively hinder grain boundary motion coupled with the relatively low temperatures for active diffusional processes.

(3) An estimated activation energy of 20 kJ/mol was found for grain coarsening in the low temperature regime (<773 K).

(4) Above 873 K the estimated activation energy shifted to 105 kJ/mol. In turn, this indicates that Ostwald-Ripening might be effective in promoting mass coarsening at high temperatures.

References

[1] D. P. Moon and M. J. Bennett, "The effects of reactive element oxide coatings on the oxidation behavior of metals and alloys at high temperatures," *Materials Science Forum*, vol. 43, pp. 269–298, 1989.

[2] E. A. Polman, T. Fransen, and P. J. Gellings, "The reactive element effect; ionic processes of grain-boundary segregation and diffusion in chromium oxide scales," *Journal of Physics: Condensed Matter*, vol. 1, no. 28, pp. 4497–4510, 1989.

[3] H. F. Lopez, "High-temperature oxidation resistant nanocoatings on austenitic stainless steels," *MRS Proceedings*, vol. 1243, pp. 21–28, 2009.

[4] H. F. Lopez and H. Mendoza-Del-Angel, "Nanoceria coatings and their role on the high temperature stability of 316L stainless steels," in *Proceedings of the 19th International Congress on Materials Research*, vol. 1276, pp. 123–128, August 2010.

[5] G. Panzera, V. Modafferi, S. Candamano, A. Donato, F. Frusteri, and P. L. Antonucci, "CO selective oxidation on ceria-supported Au catalysts for fuel cell application," *Journal of Power Sources*, vol. 135, no. 1-2, pp. 177–183, 2004.

[6] N. Izu, W. Shin, I. Matsubara, and N. Murayama, "Evaluation of response characteristics of resistive oxygen sensors based on porous cerium oxide thick film using pressure modulation method," *Sensors and Actuators B*, vol. 113, no. 1, pp. 207–213, 2006.

[7] S. Yabe and T. Sato, "Cerium oxide for sunscreen cosmetics," *Journal of Solid State Chemistry*, vol. 171, no. 1-2, pp. 7–11, 2003.

[8] F. Millot and P. D. Mierry, "A new method for the study of chemical diffusion in oxides with application to cerium oxide CeO_{2-x}," *Journal of Physics and Chemistry of Solids*, vol. 46, no. 7, pp. 797–801, 1985.

[9] P. Wynblatt and N. A. Gjostein, "Particle growth in model supported metal catalysts-I. Theory," *Acta Metallurgica*, vol. 24, no. 12, pp. 1165–1174, 1976.

[10] P. Wynblatt, R. A. Dalla Betta, and N. A. Gjostein, *The Physical Basis for Heterogeneous Catalysts*, Plenum Press, New York, NY, USA, 1975, Edited by: E. Drangles, R. I. Jafee.

[11] T. R. Malow and C. C. Koch, "Grain growth in nanocrystalline iron prepared by mechanical attrition," *Acta Materialia*, vol. 45, no. 5, pp. 2177–2186, 1997.

[12] J. A. Eastman, "Microstructural development in nanophase TiO_2 during annealing," *Journal of Applied Physics*, vol. 75, no. 2, pp. 770–779, 1994.

[13] V. K. Ivanov, O. S. Polezhaeva, G. P. Kopitsa, P. P. Fedorov, K. Pranzas, and V. V. Runov, "Specifics of high-temperature coarsening of ceria nanoparticles," *Russian Journal of Inorganic Chemistry*, vol. 54, no. 11, pp. 1689–1696, 2009.

[14] S. Patil, S. C. Kuiry, S. Seal, and R. Vanfleet, "Synthesis of nanocrystalline ceria particles for high temperature oxidation resistant coating," *Journal of Nanoparticle Research*, vol. 4, no. 5, pp. 433–438, 2002.

[15] H. Mendoza-Del-Angel, *High temperature stability of 316 austenitic stainless steel coated with CeO_2 nanoparticles [Ph.D. thesis]*, University of Wisconsin-Milwaukee, 2011.

[16] X.-D. Zhou and W. Huebner, "Size-induced lattice relaxation in CeO_2 nanoparticles," *Applied Physics Letters*, vol. 79, no. 21, pp. 3512–3514, 2001.

[17] M. J. Mayo and D. C. Hague, "Porosity-grain growth relationships in the sintering of nanocrystalline ceramics," *Nanostructured Materials*, vol. 3, no. 1-6, pp. 43–52, 1993.

[18] M. J. Mayo, D. C. Hague, and D.-J. Chen, "Processing nanocrystalline ceramics for applications in superplasticity," *Materials Science and Engineering A*, vol. 166, no. 1-2, pp. 145–159, 1993.

[19] R. S. Averback, H. J. Höfler, and R. Tao, "Processing of nanograined materials," *Materials Science and Engineering A*, vol. 166, pp. 169–177, 1993.

[20] M. J. Mayo, "Processing of nanocrystalline ceramics from ultrafine particles," *International Materials Reviews*, vol. 41, no. 3, pp. 85–115, 1996.

[21] P. G. Shewmon, *Diffusion in Solids*, John Wiley & Sons, 2nd edition, 1989.

[22] M. N. Rahaman, "Sintering and grain growth of ultrafine CeO_2 powders," in *Sintering Technology*, R. M. German, G. L. Messing, and R. Cornwall, Eds., pp. 93–100, Marcel Dekker, New York, NY, USA, 1996.

[23] G. S. A. M. Thuenissen, A. J. A. Winnbust, and A. J. Burggraaf, "Sintering kinetics and microstructure development of nanoscale Y-TZP ceramics," *Journal of the European Ceramic Society*, vol. 11, pp. 319–324, 1993.

[24] J. M. Rakowski and A. Ludlum, "High temperature oxidation of heat-resistant alloys in combustion environments," in *Proceedings of the NACE International Corrosion Conference*, 2008.